Langmuir

Article

pubs.acs.org/Langmuir

Sizing of Reverse Micelles in Microemulsions using NMR Measurements of Diffusion

Susan J. Law and Melanie M. Britton*

School of Chemistry, University of Birmingham, Edgbaston, Birmingham, B15 2TT, United Kingdom

ABSTRACT: This paper reports the size of reverse micelles (RMs) in AOT/octane/H_2O and CTAB/hexanol/H_2O microemulsions using magnetic resonance (MR) pulsed field gradient (PFG) measurements of diffusion. Diffusion data were measured using the pulsed gradient stimulated echo (PGSTE) experiment for surfactant molecules residing in the RM interface. Inverse Laplace transformation of these data generated diffusion coefficients for the RMs, which were converted into hydrodynamic radii using the Stokes−Einstein relation. This technique is complementary to those previously used to size RMs, such as dynamic light scattering (DLS) and small-angle X-ray scattering (SAXS), but also offers several advantages, which are discussed. RM sizes, determined using the PGSTE method, in the AOT (sodium bis(2-ethylhexyl) sulfosuccinate) and CTAB (cetyltrimethylammonium bromide) microemulsions were compared with previous DLS and SAXS data, showing good agreement. Methods for determining number distributions from the PGSTE data, through the use of scaling factors, were investigated.

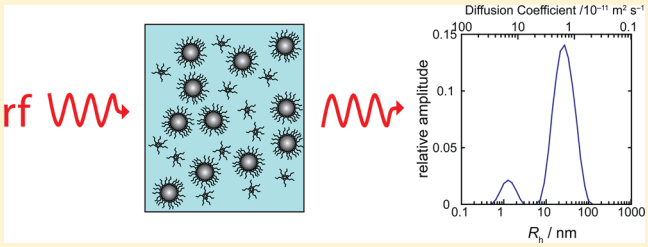

INTRODUCTION

Reverse micelles (RMs) are composed of nanosized water droplets sequestered by surfactants in a continuous organic phase. These self-assembled structures form thermodynamically stable droplets of water ranging in intramicellar diameter from approximately 1 to 20 nm, depending on the molar water-to-surfactant ratio (ω).[1] The aqueous core of RMs provides a highly adaptable environment for a variety of chemical and biochemical reactions,[2,3] protein extraction,[4] synthesis of nanoparticles,[5] as well as providing a model for biological systems.[6,7] For all of these applications, an understanding of the structure, size and polydispersity of the RMs is important, as well as an understanding of how these vary with ω and/or the presence of additional ions and molecules.

Dynamic light scattering (DLS), also known as photon correlation spectroscopy or quasi-elastic light scattering, is an extremely popular method[8] used for determining the size of RMs, as their hydrodynamic radii are typically in the submicrometer range. In DLS, the temporal fluctuations of light scattered by diffusing particles in liquid suspension are measured, which are sensitive to the diffusive motion of the particles. Analysis of the scattered light yields the diffusion coefficients (D) of the particles in suspension, which leads, where particles are spherical, to the hydrodynamic radii (R_h) using the Stokes−Einstein relation, eq 1:

$$D = k_B T/(6\pi\eta R_h) \quad (1)$$

where η is the viscosity of the pure solvent, T is the temperature, and k_B is the Boltzmann constant.

While DLS is widely used to probe the size and size distributions of submicrometer-sized particles, proteins, and RMs, it is known to have a few limitations and drawbacks.[9−12] It can struggle to find the correct particle size distributions in systems, which contain polydispersed particles or droplets, where their sizes range over several orders of magnitude. In these systems, the contribution of light scattered from smaller particles can be swamped by the light scattered by larger particles. The technique is also sensitive to the presence of dust particles, which produce bursts of high-intensity scattered light, as the larger, unwanted light-scatterers move through the illuminated sample.[10,11] Thus it becomes necessary to either completely remove all dust particles from the sample by filtration or perform additional analysis of the data.[11] However, this can sometimes require considerable effort and is sometimes not desirable or possible. Other problems arise when the dielectric constant for the droplet matches the continuous organic phase, a condition called the optical matching point, where the droplets become invisible in light scattering experiments.[13] Also, extreme caution is required in the transformation of the DLS data into number distributions, which are the distributions typically reported. DLS generates an intensity-weighted size distribution, which is converted in a volume distribution, using Mie theory[14] and then further transformed into a number distribution. Unfortunately, when using this method, small errors in data collection can lead to large errors in the number distribution[10,15] and is particularly a problem when the polydispersity of the sample is high.[16] Hence, conversion into number distributions is discouraged.[17]

An alternative method for measuring the diffusion coefficients of RMs is the magnetic resonance (MR) pulsed field gradient (PFG) experiment.[18,19] This method is known[20]

Received: February 24, 2012
Revised: July 13, 2012
Published: July 14, 2012

to provide accurate measurements of D and, while its analysis is analogous to the DLS method, requiring the inverse Laplace transform (ILT) and Stokes−Einstein relation to generate particle size distributions from diffusion measurements, it offers several advantages over DLS. First, MR methods are able to probe optically opaque or particularly turbid solutions. MR measurements are unaffected by the presence of dust particles or by the dielectric constant[13,21] of the constituents of the microemulsion. MR can also distinguish between different molecular species in a sample. A few studies have been reported in the literature[6,22−28] that measure the diffusion coefficients of RMs using PFG experiments, probing the restricted diffusion of molecules inside the emulsion droplet. These experiments have typically yielded single, averaged diffusion coefficients for the RMs by measuring the surfactant or cosurfactant signal and fitting the data to the Stejskal−Tanner relationship[29] (eq 2), which have then been converted into a single average value for the droplet size using the Stokes−Einstein relation. Droplet size distributions have been generated from PFG data for emulsions, by Ambrosone et al.[30] using a nonlinear least-squares fitting procedure and a "generating function" series. Other emulsion droplet sizing studies[31−33] use log-normal distribution fitting procedures or regularisation methods based on the distribution area or second derivative of the distribution.[34] However, to date, no studies have been reported where droplet size distributions have been determined using PFG methods for RMs in a microemulsion. Yet, PFG measurements have been successfully combined with the ILT to measure size distributions and polydispersity for polymers,[35,36] colloidal systems,[37,38] and porous media.[39]

In this paper, we demonstrate for the first time the application of PFG measurements with the ILT, to produce droplet size distributions of RMs in sodium bis(2-ethylhexyl) sulfosuccinate (AOT) and cetyltrimethylammonium bromide (CTAB) microemulsions. Using this method, we investigate the change in droplet size as a function of the water-to-surfactant ratio, ω, volume droplet fraction, ϕ_d, composition and solution age. While this paper has focused on the RMs formed using AOT or CTAB surfactants, the methods described in this paper can be readily adapted to investigate the size and distributions for a variety of micelle, RM, and microemulsion systems. These methods could also be developed into two-dimensional techniques,[40] providing insight into the dynamics of these systems, mixing of material between droplets, and the exchange of surfactant or water molecules between droplets.

EXPERIMENTAL SECTION

Reverse Micelle Preparation. A stock solution of 1.5 M AOT (Fluka, ≥96%) in *n*-octane (Acros, 97%) was prepared by dissolving 111.14 g of AOT in 70 mL of *n*-octane. Microemulsions were prepared at water-to-surfactant ratios of ω = 5.3−35 and at a droplet fraction of ϕ_d = 0.15, by adding the correct volume of water (Nanopure filtered, 18 MΩ) to the 1.5 M AOT solution to produce the required ω and diluting with *n*-octane to give ϕ_d = 0.15. By using a droplet fraction of 0.15, it is not necessary to make any correction for collisions, as would be the case in more concentrated solutions. Diffusion measurements were taken 2 h after the samples were prepared. Additional AOT microemulsions were also prepared, which included additives and were studied as a function of time and ϕ_d. The first[41,42] was prepared at ω = 15 and ϕ_d = 0.55, loaded with H_2SO_4 (Fisher >95%) = 0.4 M and malonic acid (Alfa Aesar 99%) = 0.6 M. Diffusion measurements were taken at t = 2 h and t = 24 h. The second[43] was prepared at ω = 12 and ϕ_d = 0.5, 0.4, 0.25, and 0.15, and was loaded with H_2SO_4 = 0.25 M, malonic acid = 0.25 M, and $NaBrO_3$(Alfa Aesar 99.5%) = 0.16 M. Lastly, a CTAB/hexanol/water microemulsion was prepared with CTAB (cetyltrimethylammonium bromide; Sigma ≥98%) and 1-hexanol (Acros 98%) at ω = 7.2, and ϕ_d = 0.4, giving a 3:1 w % ratio of CTAB/H_2O.[44]

Pulsed Gradient Stimulated Echo Experiments. ^{1}H NMR pulsed gradient stimulated echo (PGSTE) experiments[20] were used to measure the diffusion coefficients of the surfactant molecules in the RMs. This method applies two magnetic field gradient pulses of strength **G** and duration δ, which are separated by an observation time Δ.[45] In the case of diffusion, where molecular motion is incoherent, molecular displacements over the time scale Δ produce a distribution of phase shifts in the MR signal, resulting in an attenuation of the MR signal. The MR signal is acquired over a range of **G** values, and a diffusion coefficient can be calculated using the Stejskal−Tanner relationship:

$$\frac{S(\mathbf{G})}{S(0)} = \exp\left[-\gamma^2\delta^2\mathbf{G}^2D\left(\Delta - \frac{\delta}{3}\right)\right] \quad (2)$$

where $S(\mathbf{G})$ is the signal at gradient amplitude **G**, and $S(0)$ is the signal at zero gradient. In PGSTE experiments, a stimulated echo[20] is used, which stores the magnetization along the longitudinal axis during the relatively long observation time, making it less susceptible to T_2 relaxation. This is beneficial in samples where the T_2 is significantly shorter than T_1, which is frequently the case for protons in surfactant molecules in an RM. The stimulated echo experiment also has the advantage over the equivalent spin echo (PGSE) experiment, of not being so affected by peak distortions caused by J-coupling.[46]

PGSTE experiments were performed on a Bruker DMX300-spectrometer equipped with a 7.0 T superconducting magnet, operating at a frequency of 300.13 MHz. A 10 mm radiofrequency resonator was used, and measurements were performed at 289 ± 0.3 K. A total of 64 signal averages were collected with a repetition time of 1s. Typical parameters used in these experiments were δ = 4 ms, Δ = 100 ms, with a maximum gradient, $\mathbf{G}_{max}$, of 0.9 T m^{-1}, and 32 or 256 gradient steps, ensuring the signal attenuated so that $S(\mathbf{G})/S(0)$ at $\mathbf{G}_{max}$ was ≤0.01. The gradient system was calibrated by measuring the diffusion coefficient of *n*-octane. A value of 1.998 ± 0.01 × 10^{-9} m^2 s^{-1} was measured at 289 ± 0.3 K, which is the expected value compared to the previously reported temperature dependency of the diffusion coefficient for *n*-octane.[47] Diffusion data was collected for each system using a proton resonance that was in or near the headgroup of each surfactant. In the case of the AOT microemulsions, proton H_3 on the AOT molecule was used (Figure 1a), and, in the case of the CTAB

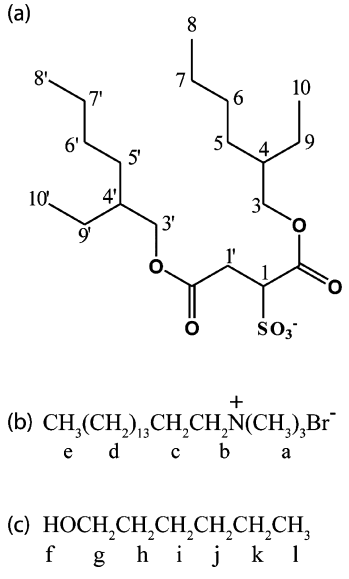

Figure 1. Molecular structure and numbering scheme for protons in the AOT (a), CTAB (b), and hexanol (c) molecules.

dx.doi.org/10.1021/la300796u | *Langmuir* 2012, 28, 11699−11706

microemulsion, proton H_a on the CTAB molecule was used (Figure 1b). Using these data, average diffusion coefficients were obtained using the Stejskal–Tanner relationship (eq 2), while diffusion coefficient distributions were determined using the ILT.[48,49] In the ILT analysis, plots of $\mathbf{G}(D)D$ vs $\log(D)$ are produced, where $\mathbf{G}(D)$ is the distribution function with respect to D. A constrained regularization ILT method[35,48−52] was used, which assumed $\mathbf{G}(D)$ was non-negative and smooth, and the noise was additive, Gaussian, and had a zero mean. The regularization parameter used was α, which measured the smoothness of $\mathbf{G}(D)$. The optimal value of α, was determined by repeating the ILT and measuring χ^2, where χ is the fit error, as a function of α.[51,52] The lowest value of α was then chosen, before χ^2 rapidly increased, corresponding to the point where the narrowest distribution was possible, without introducing spurious peaks generated by fitting the noise.[51] Typical signal-to-noise ratios, calculated as the maximum signal divided by the standard deviation of the noise, were around 65 for the H_3 peak in the AOT microemulsions and 1000 for the H_a peak in the CTAB microemulsions. Typical PGSTE diffusion data, for the H_3 peak in an AOT/octane/water microemulsion, are shown in Figure 2. Hydrodynamic radii, R_h, were

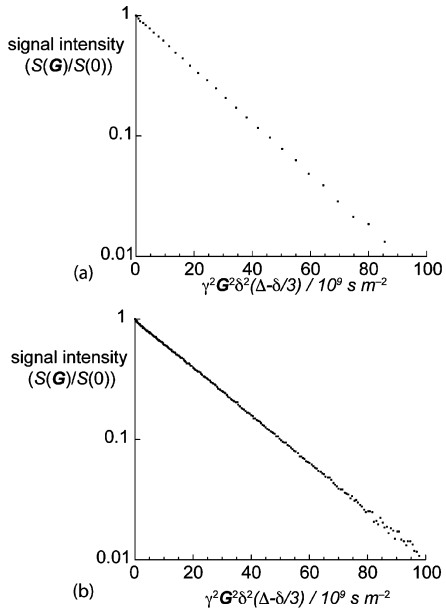

Figure 2. PGSTE diffusion data for the H_3 peak in an AOT/*n*-octane/H_2O microemulsion at $\omega = 15$ and $\phi = 0.15$, where $\Delta = 100$ ms, $\delta = 4$ ms, and $G_{max} = 0.9$ T m^{-1}. A total of 32 (a) or 256 (b) gradient steps were collected, with 64 signal averages.

determined from an average diffusion coefficient or diffusion coefficient distribution using the Stokes–Einstein relationship (eq 1). Viscosity values of 0.563 and 5.85 cP were used for *n*-octane and hexanol, respectively, at $T = 290$ K. Errors were determined from analysis of the variation between repeated experiments for a given system.

Dynamic Light Scattering. DLS measurements were performed on a Delsa-Nano Submicrometer (Class 1 Laser) Particle Size Analyzer. All solutions were filtered prior to measuring with a PTFE filter membrane (VWR). The microemulsions were allowed to equilibrate for 300 s at 290 K, and data was accumulated for 100 s with five repetitions. The time domain correlation method was used with CONTIN analysis.[48] A refractive index of 1.3975 was used for *n*-octane with a viscosity of 0.563 cP at 290 K. DLS measurements were made for the AOT/*n*-octane/H_2O samples at $\omega = 5.3 - 35$ with a droplet fraction of $\phi_d = 0.15$. The number distribution is reported.

RESULTS

^{1}H NMR spectra for the AOT/*n*-octane/water and CTAB/hexanol/water microemulsions are shown in Figure 3. These

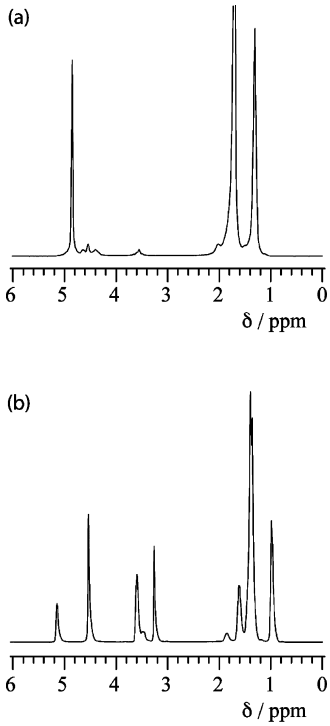

Figure 3. ^{1}H NMR spectra of AOT/*n*-octane/H_2O (a) and CTAB/hexanol/H_2O (b) microemulsions.

microemulsions have been previously characterized by NMR spectroscopy[44,53] and peak assignments for these spectra are given in Table 1 for the AOT microemulsion and Table 2 for

Table 1. ^{1}H NMR Peak Assignments for AOT/*n*-Octane/H_2O Microemulsion

peak assignments	δ/ppm
H_8, H_8', H_{10}, H_{10}', $H_{(octane)}$	1.29
H_5, H_5', H_6, H_6', H_7, H_7', H_9, H_9', $H_{(octane)}$	1.70
H_1	4.61
H_1'	3.54
H_3	4.52
H_3'	4.38
H_4, H_4'	1.99
H_2O	4.84

Table 2. ^{1}H NMR Peak Assignments for CTAB/Hexanol/H_2O Microemulsion

peak assignments	δ/ppm
H_f	5.09
H_2O	4.48
H_g	3.54
H_b	3.42
H_a	3.22
H_c	1.79
H_h	1.56
H_d, H_i, H_j, H_k,	1.34
H_e, H_l	0.94

dx.doi.org/10.1021/la300796u | *Langmuir* 2012, 28, 11699−11706

the CTAB microemulsion. Figure 4a gives the average diffusion coefficients for AOT surfactant molecules in the AOT/*n*-

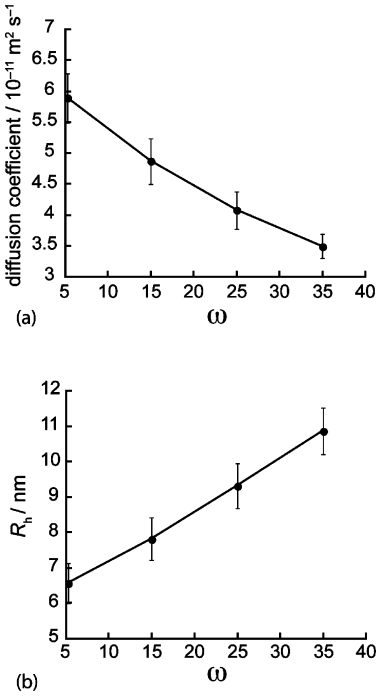

Figure 4. Plots of the average diffusion coefficient (a) and hydrodynamic radii (b) for RMs in AOT/*n*-octane/H_2O microemulsions, at varying ω and ϕ_d = 0.15. The diffusion coefficients were determined using the 32 gradient step PGSTE data from the H_3 proton on the AOT headgroup and fitted to the Stejskal–Tanner equation.

octane/water system, following fitting of the PGSTE data to the Stejskal–Tanner equation (eq 2). As the surfactant molecule resides in the interface of the RM, these diffusion coefficients provide a measure of the diffusion coefficient of the RM. By using the Stokes–Einstein relation (eq 1), droplet sizes for the RMs were calculated, as a function of ω, and are presented in Figure 4b. Analysis of the DLS data for the samples reported in Figure 4 gave average droplet sizes of 1.2 ± 0.3 nm at ω = 5.3; 1.65 ± 0.5 nm at ω = 15; 3.15 ± 0.8 nm at ω = 25 and 3.9 ± 1.1 nm at ω = 35.

ILT of PGSTE data produces a distribution of diffusion coefficients (Figure 5a), which have been converted into a distribution of molecular sizes (Figure 5b,c) using the Stokes–Einstein equation (eq 1). Analysis of the distribution maxima for the 32 gradient step (Figure 5b) PGSTE data produced R_h values of 6.5 ± 0.5 nm at ω = 5.3; 7.5 ± 0.7 nm at ω = 15; 9.1 ± 0.8 nm at ω = 25; and 11.8 ± 2 nm at ω = 35. R_h values for the 256 gradient step (Figure 5c) PGSTE experiments yielded values of 6.3 ± 0.5 nm at ω = 5.3; 7.8 ± 0.7 nm at ω = 15; 8.9 ± 0.8 nm at ω = 25; and 14.7 ± 2 nm at ω = 35.

The effect of additives on the size and stability of RMs was investigated by measuring diffusion coefficients and determining droplet size distributions for two AOT/*n*-octane/water microemulsions loaded with H_2SO_4 (0.4 M) and malonic acid (0.6 M)[42] or H_2SO_4 (0.25 M), malonic acid (0.25 M), and BrO_3^- (0.16 M)[43] as a function of time and droplet fraction, respectively. These systems are known[42,43] to produce bimodal droplet size distributions, which become unimodal after time[42] ($t \geq 24$ h) or lower droplet fraction[43] ($\phi_d < 0.5$). Droplet size

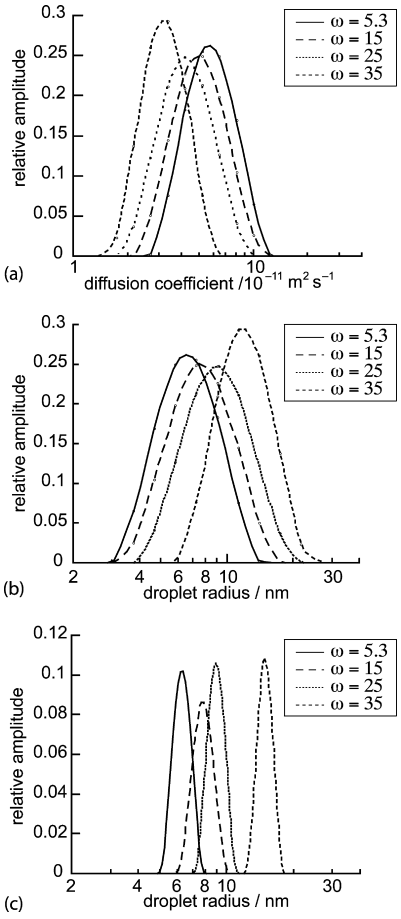

Figure 5. Plots of the diffusion coefficient distributions (a) and droplet size distributions using 32 gradient steps (b) and 256 gradient steps (c) for RMs at varying ω in AOT/*n*-octane/H_2O microemulsions at ϕ_d = 0.15. The diffusion coefficients were determined using the PGSTE data for the H_3 proton on the AOT headgroup, using the ILT. RM size distributions were generated from the diffusion coefficient distributions using the Stokes–Einstein relation.

distributions determined using PGSTE measurements are presented in Figure 6 for the system previously investigated by Vanag et al.[42] for fresh and 24 h old samples. Figure 7 shows the size distributions of RMs in the system previously investigated by Alvarez et al.,[43] at varying droplet fractions.

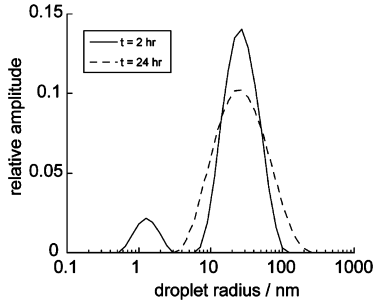

Figure 6. Droplet size distributions for RMs in the AOT/*n*-octane/H_2O microemulsion loaded with [H_2SO_4] = 0.4 M and [malonic acid] = 0.6 M at ω = 15 and ϕ_d = 0.55 at 2 and 24 h after preparation. Size distributions were produced by applying the Stokes–Einstein relation to diffusion coefficient distributions produced by ILT of the PGSTE data for AOT H_3 proton. 32 gradient steps were used.

dx.doi.org/10.1021/la300796u | *Langmuir* 2012, 28, 11699–11706

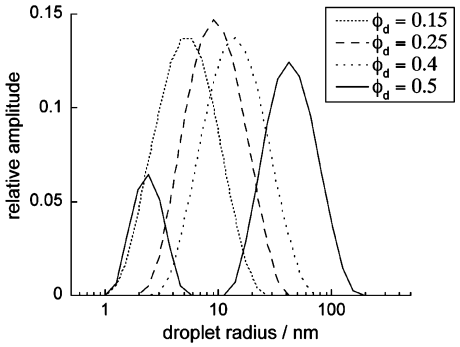

Figure 7. Droplet size distributions for RMs in the AOT/*n*-octane/H_2O microemulsion loaded with [H_2SO_4] = 0.25 M, [malonic acid] = 0.25, and 0.16 M [$NaBrO_3$] at ω = 12, at ϕ_d = 0.15−0.5. Size distributions were produced by applying the Stokes−Einstein relation to diffusion coefficient distributions produced by inverse Laplace transformation of the PGSTE data for AOT H_3 proton. 32 gradient steps were used.

Finally, the diffusion coefficients and droplet size distributions for the CTAB/hexanol/water microemulsion (ω = 7.2 and ϕ_d = 0.4) determined using PGSTE experiments, are presented in Figure 8. A droplet size of 0.9 nm was determined from the droplet size distribution.

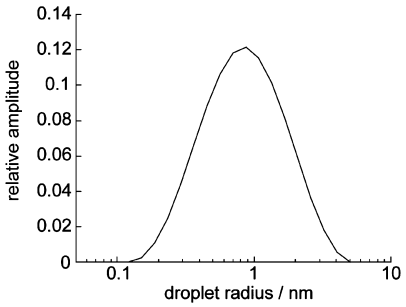

Figure 8. Droplet size distribution for RMs in a CTAB/hexanol/H_2O microemulsion at ω = 7.2 and ϕ_d = 0.4. Size distributions were produced by applying the Stokes−Einstein relation to diffusion coefficient distributions produced by inverse Laplace transformation of the PGSTE data for CTAB H_a proton. 32 gradient steps were used.

DISCUSSION

Comparison of the RM size distributions using 32 or 256 gradients steps shows good agreement between the R_h values produced. Yet, it can be seen, when comparing panels b and c of Figure 5, that the width of the distribution is dependent on the number of gradient steps acquired. As the width of the distributions are sensitive to the number of gradient steps collected, as well as the parameters used in the ILT, such as the α value, we do not suggest that these results can be used to determine the polydispersity of the RMs. However, even though the distribution widths are seen to change, the R_h values were not found to change significantly with these.

Comparisons between our R_h values were made with those previously reported. RMs in AOT/octane/water microemulsions are some of the most studied in the literature, with a number of papers reporting their size using DLS,[54−59] small-angle X-ray scattering (SAXS),[60−62] and fluorescence correlation spectroscopy (FCS),[13] as a function or ω and ϕ_d. The sizes typically reported using these methods are on the order of 2.5−9.5 nm for ω values of 5−35 (Figure 9). By comparing our PGSTE-determined droplet sizes with our DLS data and the

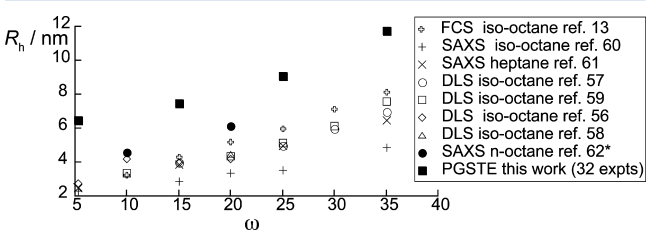

Figure 9. Plot of droplet size (R_h) dependence on ω for values reported in the literature using DLS,[56−59] FCS,[13] and SAXS[60−62] methods. *The values given for R_h were determined using the r_w value reported in ref 62 with 2 × 1.5 nm added to account for the width of the surfactant layer around the water core.

data previously reported, it is clear that our hydrodynamic radii are larger. The origins of these differences are, as yet, unclear. These discrepancies could lie in errors in the PGSTE data associated with exchange of surfactant molecules, during the observation time (Δ), between droplets of difference sizes. However, as previous investigations of AOT/octane/water microemulsions do not indicate the presence of larger RMs, it seems unlikely that the error can arise simply from exchange. It is possible that differences between PGSTE and DLS methods could lie in the errors introduced during the conversion of DLS data to number distributions. Indeed, the use of number distributions is discouraged,[17] although they are frequently reported in the literature. Yet, this does not explain why our values are larger than those determined by FCS and some SAXS studies. Further investigation is required.

While our droplet sizes for the AOT/octane/water microemulsions are larger than those previously reported, our values for the microemulsions containing additives actually compare well. In these systems, bimodal size distributions are produced, as have been previously observed[42,43] in DLS measurements. In the system studied by Vanag et al.,[42] the bimodal behavior was observed in fresh samples, which become unimodal with time. This behavior is also observed in the PGSTE data. In the fresh sample, there were peaks at 1.3 and 25.8 nm, which compares closely with the values observed by Vanag et al. of 2 and 20 nm. At 24 h after mixing, the sample was unimodal, with an average droplet size of 25.1 nm. This value is, however, significantly higher than that observed by DLS, which measured a size distribution centered at 3.6 nm. In the system previously studied by Alvarez et al., a transition from bimodal to unimodal size distributions was observed as a function of volume fraction, rather than time. Bimodal behavior was observed at a ϕ_d value of 0.5, with R_h values of 2.4 and 42.1 nm for the two peaks. This behavior was previously observed by DLS, with peaks centered at 2−3 nm and 20−30 nm.[43] As ϕ_d was reduced, the system became unimodal, and droplet sizes of 13.8 nm (ϕ_d = 0.40), 9.1 nm (ϕ_d = 0.25) and 5.2 nm (ϕ_d = 0.15) were observed. Unimodal distributions have also been observed by DLS; however, the peak for the distribution presented in ref 43 was lower at 2−3 nm, although the volume fraction for the data was not reported.

While the RM sizes show general agreement with previous DLS measurements, there are differences with the distribution of droplets. The origins of this lie in how the diffusion coefficients of the RMs are determined and what the PGSTE measures. Just as DLS measures intensity distributions, which

dx.doi.org/10.1021/la300796u | *Langmuir* 2012, 28, 11699−11706

are then converted into number distributions, so PGSTE data should also be scaled to produce a number distribution of droplet sizes. Such scaling is necessary where the droplet size ranges corresponded to a range of droplets containing different amounts of surfactant molecules. Thus, if larger droplets contain greater numbers of surfactant molecules, it is necessary to take this into account. Hence, the droplet size distributions need to be scaled in order to produce a number distribution.

In our experiments, droplet sizes are determined from diffusion coefficients calculated from the PGSTE data of the surfactant molecules, which are dominated by the diffusion rate of the RM (where all surfactant molecules are located in the RM). The surfactant molecules surround the water core of the RM, so their number, N_s, is expected to increase proportionally with r_w^2, where r_w is the radius of the water core. As the PGSTE signal is integrated over all surfactant molecules, it means that surfactant molecules in larger droplets will contribute more to the distribution of diffusion coefficients than smaller droplets. In order to correct the droplet size distributions for this, it is necessary to divide the relative amplitude by the number of surfactant molecules, N_s, contributing to the PGSTE decay for each droplet size (R_h). Calculation of N_s provides a method for scaling the PGSTE data, leading to a number distribution of RM droplet sizes. In order to determine N_s, the size of the droplet core, r_w, was first calculated for each value of R_h using eq 3 and a value of 1.5 nm for δ, the thickness of the surfactant layer.[13]

$$R_h = (r_w^3 + 3\delta r_w^2)^{1/3} \quad (3)$$

Using the size parameters determined previously[54,63] for the AOT/iso-octane/water system (Table 3), N_s was determined,

Table 3. Size Parameters for the AOT/Iso-octane/Water System Taken from Ref 54

ω	N_s	R_h/nm	r_w/nm
4	35	2.5	1.0
6	50	2.8	1.4
8	72	3.2	1.6
10	98	3.4	1.9
12	129	3.7	2.2
14	176	4.0	2.6
16	215	4.2	2.9
18	257	4.3	3.2
20	302	4.4	3.5
25	447	5.2	4.3
30	613	6.2	5.1
35	778	7.6	5.8

as a function of r_w, for each value of R_h in the droplet size distributions. Number distributions were then generated by dividing the relative amplitude by N_s at each value of R_h. A limitation with this method, however, is that it requires prior characterization of the system. An alternative method to scale the distributions would be to simply use r_w^2 as a scaling factor and include an offset to take into account the surfactant aggregation number in the absence of water. Previous studies have determined the aggregation number for AOT in iso-octane to be 22.[64] Using this, number distributions were produced by scaling the data by $(r_w^2 + 22)$. This scaling, however, assumes that the area (a_s) occupied by the surfactant headgroup at the water core interface remains constant over the range of droplet sizes observed, an assumption made by other studies.[13,21]

Using both N_s and $(r_w^2 + 22)$ scaling methods, number distributions were produced for the AOT microemulsions containing additives, which are presented in Figure 10. These

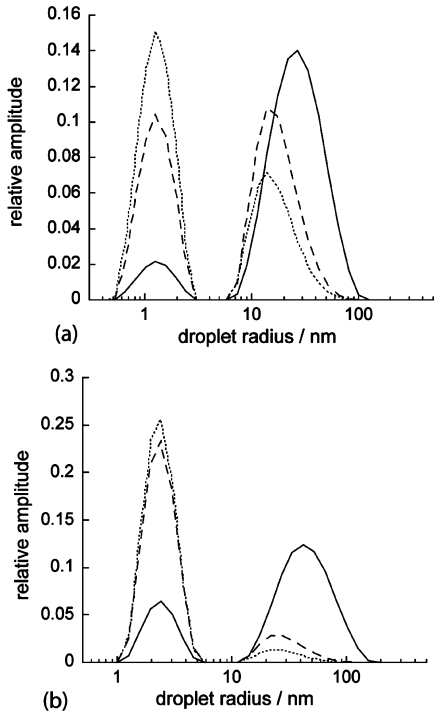

Figure 10. Droplet size distribution for RMs in an AOT/*n*-octane/H_2O microemulsion loaded with (a) $[H_2SO_4]$ = 0.4 M and [malonic acid] = 0.6 M at ω = 15 and ϕ_d = 0.55 (unscaled data from Figure 6) and (b) $[H_2SO_4]$ = 0.25 M, [malonic acid] = 0.25 and 0.16 M $[NaBrO_3]$ at ω = 12 and ϕ_d = 0.5 (unscaled data from Figure 7). R_h values are given for data that is unscaled (——), scaled by N_s (- - - -), and scaled by $(r_w^2 + 22)$ (·····).

distributions now show a higher proportion of smaller droplets, compared to the unscaled distributions. The average RM sizes for each mode are also slightly smaller. It should be noted that this method of scaling may not be applicable in these systems, as it assumes the larger droplets are also spherical, which may not be the case. Further work is required to determine which is the most appropriate scaling for these systems. However, regardless of the precise details of the scaling used, our method for determining number distributions of RMs in microemulsions has advantages over the methods used for determining size distributions in macroemulsions, which probe the restricted diffusion of molecules contained inside the droplets and hence require a scaling proportional to a^3, where a is the droplet radius.[34]

The need for a scaling factor also has further implications for the accuracy of average diffusion coefficients calculated using the Stejskal–Tanner equation, and their use in determining droplet sizes in multimodal systems. While the use of average diffusion coefficients may be sufficient to determine R_h for unimodal systems, they will struggle in multimodal systems. In multimodal systems, the signal from surfactant molecules in larger droplets will contribute more toward the diffusion data than molecules from smaller droplets. In the Stejskal-Tanner analysis, relative contributions are not produced as a function of

dx.doi.org/10.1021/la300796u | *Langmuir* 2012, 28, 11699–11706

droplet size, therefore, there is no mechanism by which the data can be directly scaled, particularly without prior knowledge of the droplet size distribution. Thus, this shows that MR measurements of average diffusion coefficients, should be treated with caution for multimodal systems.

The last system investigated using this method was the CTAB/hexanol/water microemulsion. While this microemulsion has been widely studied in the literature, droplet sizes of RMs in this system have been significantly less well characterized than AOT microemulsions. In this system, R_h was calculated to be 0.9 nm, which compares well with previous droplet size measurements,[65] where a droplet size of 1.1 nm was measured for a CTAB/hexanol/water microemulsion (2.6:1 ratio % wt of CTAB/H_2O)).

CONCLUSION

In this paper, we report the first application of MR measurements of diffusion to produce, using the ILT and Stokes−Einstein relation, droplet size distributions for RMs in AOT and CTAB microemulsions. Our measurements are complementary to the methods previously used to size RMs and yield values similar to those produced by DLS. However, RM sizes in the AOT/*n*-octane/water microemulsion were found to be larger compared to those measured by optical methods, particularly at lower ω values. While we do not suggest that our data should be used to determine the polydispersity of RM sizes, it may be possible to use these methods to compare changes in size distributions as a function of ω, ϕ_d, or composition. Scaling factors were investigated that enabled number distributions to be generated and, when used, were shown to shift the distributions toward smaller droplet sizes, reducing the average droplet size. The suitability and need for these scaling factors, however, needs further investigation.

Finally, while this paper has focused on MR methods to measure RM sizes, we would like to add that these experiments can easily be adapted into two-dimensional techniques, such as diffusion-relaxation correlation spectroscopy (DRCOSY)[66] and diffusion−diffusion exchange spectroscopy (DEXSY).[40] In these experiments, data is acquired in two-dimensions, followed by two-dimensional Laplace transformation,[52] enabling correlations between diffusion and relaxation behavior, for either surfactant or water molecules, which could lead to greater insight into the behavior of these dynamic structures.

AUTHOR INFORMATION

Corresponding Author

*E-mail address: m.m.britton@bham.ac.uk.

Notes

The authors declare no competing financial interest.

ACKNOWLEDGMENTS

The authors thank the reviewers for probing comments, which have been helpful in the development of this work, and EPSRC and the University of Birmingham for funding. The Delsa Nano Beckman-Coulter DLS instrument used in this research was obtained, through Birmingham Science City: Innovative Uses for Advanced Materials in the Modern World (West Midlands Centre for Advanced Materials Project 2), with support from Advantage West Midlands (AWM) and partly funded by the European Regional Development Fund (ERDF).

REFERENCES

(1) De, T. K.; Maitra, A. Solution behavior of Aerosol OT in nonpolar-solvents. *Adv. Colloid Interface Sci.* **1995**, *59*, 95−193.
(2) Fendler, J. H. Interactions and reactions in reversed micellar systems. *Acc. Chem. Res.* **1976**, *9*, 153−161.
(3) Pileni, M. P. Reverse micelles as microreactors. *J. Phys. Chem.* **1993**, *97*, 6961−6973.
(4) Cöklen, K. E.; Hatton, T. A. Protein extraction using reverse micelles. *Biotechnol. Prog.* **1985**, *1*, 69−74.
(5) Uskokovic, V.; Drofenik, M. Synthesis of materials within reverse micelles. *Surf. Rev. Lett.* **2005**, *12*, 239−277.
(6) Fedotov, V. D.; Zuev, Y. F.; Archipov, V. P.; Idiyatullin, Z. S.; Garti, N. A Fourier transform pulsed-gradient spin echo nuclear magnetic resonance self-diffusion study of microemulsions and the droplet size determination. *Colloids Surf., A* **1997**, *128*, 39−46.
(7) Levinger, N. E. Water in confinement. *Science* **2002**, *298*, 1722−1723.
(8) Schatzel, K. Light-scattering - Diagnostic methods for colloidal dispersions. *Adv. Colloid Interface Sci.* **1993**, *46*, 309−332.
(9) Filipe, V.; Hawe, A.; Jiskoot, W. Critical evaluation of nanoparticle tracking analysis (NTA) by NanoSight for the measurement of nanoparticles and protein aggregates. *Pharm. Res.* **2010**, *27*, 796−810.
(10) Provder, T. *Particle Size Distribution: Assessment and Characterization*; American Chemical Society: Washington, DC, 1987.
(11) Ruf, H. Treatment of contributions of dust to dynamic light scattering data. *Langmuir* **2002**, *18*, 3804−3814.
(12) Ruf, H.; Gould, B. J.; Haase, W. The effect of nonrandom errors on the results from regularized inversions of dynamic light scattering data. *Langmuir* **2000**, *16*, 471−480.
(13) Pal, N.; Verma, S. D.; Singh, M. K.; Sen, S. Fluorescence correlation spectroscopy: An efficient tool for measuring size, size-distribution and polydispersity of microemulsion droplets in solution. *Anal. Chem.* **2011**, *83*, 7736−7744.
(14) De Vos, C.; Deriemaeker, L.; Finsy, R. Quantitative assessment of the conditioning of the inversion of quasi-elastic and static light scattering data for particle size distributions. *Langmuir* **1996**, *12*, 2630−2636.
(15) Finsy, R. Particle sizing by quasi-elastic light-scattering. *Adv. Colloid Interface Sci.* **1994**, *52*, 79−143.
(16) Patty, P. J.; Frisken, B. J. Direct determination of the number-weighted mean radius and polydispersity from dynamic light-scattering data. *Appl. Opt.* **2006**, *45*, 2209−2216.
(17) ASTM Standard E2490, 2009. Standard Guide for Measurement of Particle Size Distribution of Nanomaterials in Suspension by Photon Correlation Spectroscopy (PCS). ASTM International: West Conshohocken, PA, 2009; DOI: 10.1520/E2490-09; www.astm.org.
(18) Lindman, B.; Stilbs, P.; Moseley, M. E. Fourier-transform NMR self-diffusion and microemulsion structure. *J. Colloid Interface Sci.* **1981**, *83*, 569−582.
(19) Stilbs, P.; Moseley, M. E. Multicomponent self-diffusion measurement by the pulsed-gradient spin-echo method on standard fourier-transform NMR spectrometers. *Chem. Scr.* **1980**, *15*, 176−179.
(20) Callaghan, P. T. *Principles of Nuclear Magnetic Resonance Microscopy*; Oxford University Press: Oxford, 1991.
(21) Ricka, J.; Borkovec, M.; Hofmeier, U. Coated droplet model of microemulsions - Optical matching and polydispersity. *J. Chem. Phys.* **1991**, *94*, 8503−8509.
(22) Caboi, F.; Capuzzi, G.; Baglioni, P.; Monduzzi, M. Microstructure of Ca-AOT/water/decane w/o microemulsions. *J. Phys. Chem. B* **1997**, *101*, 10205−10212.
(23) Dahirel, V.; Ancian, B.; Jardat, M.; Meriguet, G.; Turq, P.; Lequin, O. What can be learnt from the comparison of multiscale brownian dynamics simulations, nuclear magnetic resonance and light scattering experiments on charged micelles? *Soft Matter* **2010**, *6*, 517−525.
(24) Gradzielski, M. Recent developments in the characterisation of microemulsions. *Curr. Opin. Colloid Interface Sci.* **2008**, *13*, 263−269.

(25) Hedin, N.; Furo, I. Ostwald ripening of an emulsion monitored by PGSE NMR. *Langmuir* **2001**, *17*, 4746−4752.
(26) Knackstedt, M. A.; Ninham, B. W.; Monduzzi, M. Diffusion in model disordered media. *Phys. Rev. Lett.* **1995**, *75*, 653−656.
(27) Lasic, S.; Aslund, I.; Oppel, C.; Topgaard, D.; Soderman, O.; Gradzielski, M. Investigations of vesicle gels by pulsed and modulated gradient NMR diffusion techniques. *Soft Matter* **2011**, *7*, 3947−3955.
(28) Walderhaug, H.; Johannessen, E. Partition equilibria for alcohols in reverse micellar AOT-oil-water systems studied by PGSE-FT NMR. A comparison between AOT-containing and the corresponding AOT-free systems. *J. Sol. Chem.* **2006**, *35*, 979−989.
(29) Stejskal, E. O.; Tanner, J. E. Spin Diffusion Measurements: Spin Echoes in the Presence of a Time-Dependent Field Gradient. *J. Chem. Phys.* **1965**, *42*, 288−292.
(30) Ambrosone, L.; Ceglie, A.; Colafemmina, G.; Palazzo, G. A novel approach for determining the droplet size distribution in emulsion systems by generating function. *J. Chem. Phys.* **1997**, *107*, 10756−10763.
(31) Fourel, I.; Guillement, J. P.; Lebotlan, D. Determination of water droplet size distributions by low-resolution PFG-NMR. *J. Colloid Interface Sci.* **1994**, *164*, 48−53.
(32) Packer, K. J.; Rees, C. Pulsed NMR studies of restricted diffusion 1. Droplet size distributions in emulsions. *J. Colloid Interface Sci.* **1972**, *40*, 206.
(33) Johns, M. L.; Hollingsworth, K. G. Characterisation of emulsion systems using NMR and MRI. *Prog. Nucl. Magn. Reson. Spectrosc.* **2007**, *50*, 51−70.
(34) Hollingsworth, K. G.; Johns, M. L. Measurement of emulsion droplet sizes using PFG NMR and regularization methods. *J. Colloid Interface Sci.* **2003**, *258*, 383−389.
(35) Chen, A.; Wu, D. H.; Johnson, C. S. Determination of molecular weight distributions for polymers by diffusion-ordered NMR. *J. Am. Chem. Soc.* **1995**, *117*, 7965−7970.
(36) Vieville, J.; Tanty, M.; Delsuc, M. A. Polydispersity index of polymers revealed by DOSY NMR. *J. Magn. Reson.* **2011**, *212*, 169−173.
(37) Griffiths, P. C.; Cheung, A. Y. F.; Davies, J. A.; Paul, A.; Tipples, C. N.; Winnington, A. L. Probing interactions within complex colloidal systems using PGSE-NMR. *Magn. Reson. Chem.* **2002**, *40*, S40−S50.
(38) Valentini, M.; Vaccaro, A.; Rehor, A.; Napoli, A.; Hubbell, J. A.; Tirelli, N. Diffusion NMR spectroscopy for the characterization of the size and interactions of colloidal matter: The case of vesicles and nanoparticles. *J. Am. Chem. Soc.* **2004**, *126*, 2142−2147.
(39) Song, Y.-Q. Using Internal Magnetic Fields to Obtain Pore Size Distributions of Porous Media. *Con. Magn. Reson. A* **2003**, *18A*, 97−110.
(40) Callaghan, P. T.; Godefroy, S.; Ryland, B. N. Use of the second dimension in PGSE NMR studies of porous media. *Magn. Reson. Imag.* **2003**, *21*, 243−248.
(41) Vanag, V. K. Waves and patterns in reaction-diffusion systems. Belousov−Zhabotinsky reaction in water-in-oil microemulsions. *Phys. Usp.* **2004**, *47*, 923−941.
(42) Vanag, V. K.; Epstein, I. R. Dash waves in a reaction-diffusion system. *Phys. Rev. Lett.* **2003**, *90*, 098301.
(43) Alvarez, E. V.; Carballido-Landeira, J.; Guiu-Souto, J.; Taboada, P.; Munuzuri, A. P. Modulation of volume fraction results in different kinetic effects in Belousov−Zhabotinsky reaction confined in AOT-reverse microemulsion. *J. Chem. Phys.* **2011**, *134*, 094512.
(44) Halliday, N. A.; Peet, A. C.; Britton, M. M. Detection of pH in microemulsions, without a probe molecule, using magnetic resonance. *J. Phys. Chem. B* **2010**, *114*, 13745−13751.
(45) Britton, M. M. Magnetic resonance imaging of chemistry. *Chem. Soc. Rev.* **2010**, *39*, 4036−4043.
(46) Torres, A. M.; Dela Cruz, R.; Price, W. S. Removal of J-coupling peak distortion in PGSE experiments. *J. Magn. Reson.* **2008**, *193*, 311−316.
(47) Tofts, P. S.; Lloyd, D.; Clark, C. A.; Barker, G. J.; Parker, G. J. M.; McConville, P.; Baldock, C.; Pope, J. M. Test liquids for quantitative MRI measurements of self-diffusion coefficient in vivo. *Magn. Reson. Med.* **2000**, *43*, 368−374.
(48) Provencher, S. W. A Constrained Regularization Method for Inverting Data Represented by Linear Algebraic or Integral-Equations. *Comput. Phys. Commun.* **1982**, *27*, 213−227.
(49) Provencher, S. W. Contin - A general-purpose constrained regularization program for inverting noisy linear algebraic and integral-equations. *Comput. Phys. Commun.* **1982**, *27*, 229−242.
(50) Borgia, G. C.; Brown, R. J. S.; Fantazzini, P. Uniform-penalty inversion of multiexponential decay data. *J. Magn. Reson.* **1998**, *132*, 65−77.
(51) Fordham, E. J.; Sezginer, A.; Hall, L. D. Imaging multi-exponential relaxation in the (y, $\log_e T_1$) plane, with application to clay filtration in rock cores. *J. Magn. Reson., Ser. A* **1995**, *113*, 139−150.
(52) Song, Y. Q.; Venkataramanan, L.; Hurlimann, M. D.; Flaum, M.; Frulla, P.; Straley, C. T_1−T_2 correlation spectra obtained using a fast two-dimensional Laplace inversion. *J. Magn. Reson.* **2002**, *154*, 261−268.
(53) Binks, D. A.; Spencer, N.; Wilkie, J.; Britton, M. M. Magnetic resonance studies of a redox probe in a reverse sodium bis(2-ethylhexyl)sulfosuccinate/octane/water microemulsion. *J. Phys. Chem. B* **2010**, *114*, 12558−12564.
(54) Maitra, A. Determination of size parameters of water-aerosol OT-oil reverse micelles from their nuclear magnetic-resonance data. *J. Phys. Chem.* **1984**, *88*, 5122−5125.
(55) Zulauf, M.; Eicke, H. F. Inverted micelles and microemulsions in the ternary-system H_2O/aerosol-OT/isooctane as studied by photon correlation spectroscopy. *J. Phys. Chem.* **1979**, *83*, 480−486.
(56) Vasquez, V. R.; Williams, B. C.; Graeve, O. A. Stability and comparative analysis of AOT/water/isooctane reverse micelle system using dynamic light scattering and molecular dynamics. *J. Phys. Chem. B* **2011**, *115*, 2979−2987.
(57) Baruah, B.; Roden, J. M.; Sedgwick, M.; Correa, N. M.; Crans, D. C.; Levinger, N. E. When is water not water? Exploring water confined in large reverse micelles using a highly charged inorganic molecular probe. *J. Am. Chem. Soc.* **2006**, *128*, 12758−12765.
(58) Nazario, L. M. M.; Hatton, T. A.; Crespo, J. P. S. G. Nonionic cosurfactants in AOT reversed micelles: Effect on percolation, size, and solubilization site. *Langmuir* **1996**, *12*, 6326−6335.
(59) Wong, M.; Thomas, J. K.; Nowak, T. Structure and state of H_2O in reversed micelles. *J. Am. Chem. Soc.* **1977**, *99*, 4730−4736.
(60) Liu, J. C.; Li, G. Z.; Han, B. X. Characteristics of AOT microemulsion structure: A small angle X-ray scattering study. *Chin. Chem. Lett.* **2001**, *12*, 1023−1026.
(61) Hirai, M.; Hirai, R. K.; Iwase, H.; Arai, S.; Mitsuya, S.; Takeda, T.; Seto, H.; Nagao, M. Dynamics of w/o AOT microemulsions studied by neutron spin echo. *J. Phys. Chem. Solids* **1999**, *60*, 1359−1361.
(62) Balakrishnan, S.; Javid, N.; Weingartner, H.; Winter, R. Small-angle X-ray scattering and near-infrared vibrational spectroscopy of water confined in aerosol-OT reverse micelles. *ChemPhysChem* **2008**, *9*, 2794−2801.
(63) Eicke, H. F.; Rehak, J. Formation of Water/Oil-Microemulsions. *Helv. Chim. Acta* **1976**, *59*, 2883−2891.
(64) Tovstun, S. A.; Razumov, V. F. On the composition fluctuations of reverse micelles. *J. Colloid Interface Sci.* **2010**, *351*, 485−492.
(65) Rodenas, E.; Valiente, M. The determination of some physical-properties of reverse CTAB micelles in 1-hexanol. *Colloids Surf.* **1992**, *62*, 289−295.
(66) Graham, R. G.; Holmes, W. M.; De Panfilis, C.; Packer, K. J. Characterisation of locally anisotropic structures within isotropic porous solids using 2-D pulsed field gradient NMR. *Chem. Phys. Lett.* **2000**, *332*, 319−323.